The Dominant Role of Polymer Erosion in Paclitaxel Release from Folate-Modified Poly(ether-anhydride) Nanocarrier

Xipan Liu, Dan Pan, Qian Guo, Yanjun Zhao, Zheng Wang

Tianjin Key Laboratory for Modern Drug Delivery and High Efficiency, School of Pharmaceutical Science and Technology, Tianjin University, 92 Weijin Road, Tianjin 300072, China
Correspondence to: Y. Zhao (E-mail: zhaoyj@tju.edu.cn) or Z. Wang (E-mail: wangzheng2006@tju.edu.cn)

ABSTRACT: This study designed a photo-crosslinkable poly(ether-anhydride) nanocarrier with folate modification to achieve both biodegradability and active targeting. The nanocarrier consists of a hydrophobic polymer core and a shell of folate and hydrophilic poly(ethylene glycol). Nuclear magnetic resonance and Fourier transform infrared spectroscopy were used to verify the synthesis and relevant intermediate products. The nanocarrier was characterized in terms of morphology and diameter using transmission electron microscopy and dynamic light scattering. The results showed that the size of spherical nanocarriers located within 200–400 nm. The cellular uptake profile of nanocarriers in HeLa cells was examined using fluorescence microscope with the help of a fluorescent molecule and the folate-modified nanocarrier exhibited an enhanced uptake compared to that without modification. The nanocarrier degradation at physiological temperature was investigated gravimetrically and the *in vitro* release of model drug, paclitaxel (PTX) was examined via the dialysis method. The erosion rate of poly(ether-anhydride) network was controlled by the crosslinking density and the hydrolytic susceptibility; the folate modification slightly slowed the degradation process. The time scale of PTX release perfectly matched with that of nanocarrier erosion; after 6 h more than 50% weight loss of nanocarrier was observed and meanwhile the drug release profile got plateaued, indicating the dominant role of polymer erosion in the release of the active agent from the nanocarriers. © 2012 Wiley Periodicals, Inc. J. Appl. Polym. Sci. 129: 748–755, 2013

INTRODUCTION

Site-specific drug delivery to the tumour via nanocarriers has been popular because this approach can enhance the distribution and retention of chemotherapeutic agent at the tumor cells efficiently and thus reduce the toxicity to the normal cells.[1,2] Nanoparticulate anticancer drugs can be delivered to the tumor cells passively or actively. Passive targeting often takes the advantage of the leaky vasculature of tumor (e.g. the enhanced permeability and retention effect) to direct the carrier/drug to the target site.[3,4] Active targeting is based on the ligand–receptor binding and the corresponding receptor at the target site can facilitate carrier/drug to reach the specific cells.[5] Targeting via folate receptor is a common approach for delivering drugs to the tumor as the level of folate receptor in normal tissues are low, but that in tumor tissues are high due to the overexpression. The attractiveness of folate has been further enhanced by its high-binding affinity, low immunogenicity, ease of modification, stability during storage, and low cost.[6,7] Therefore, folate has been used as a targeting moiety attached to a variety of

nanocarriers including liposomes, micelles, polymeric nanoparticles, and so on to avoid the nonspecific attacks to the normal tissues and promote the cellular uptake of active agents within target cells.[8,9]

Biological stability is one of the key factors that determine the performance of nanocarriers designed for tumor targeting.[10] Micelles composed of hydrophobic and hydrophilic segments will self-assemble into core-shell structures. However, the disruption of micelles caused by binding with proteins in the blood stream and dilution into body fluids below critical micelle concentration lead to burst-release of the entrapped drugs, and the aggregation of micelles during storage also limits their application as drug carrier.[11] Liposomes also exhibit poor stability on administration; the destabilization of liposomes in blood is mainly due to the lipid exchange between liposomes and high-density lipoproteins, which leads to drug leakage before reaching the target sites.[12] In contrast, the serum stability of PEGylated polymeric nanocarriers is outstanding. Our previous work synthesized a novel type of photo-crosslinked poly(ether-
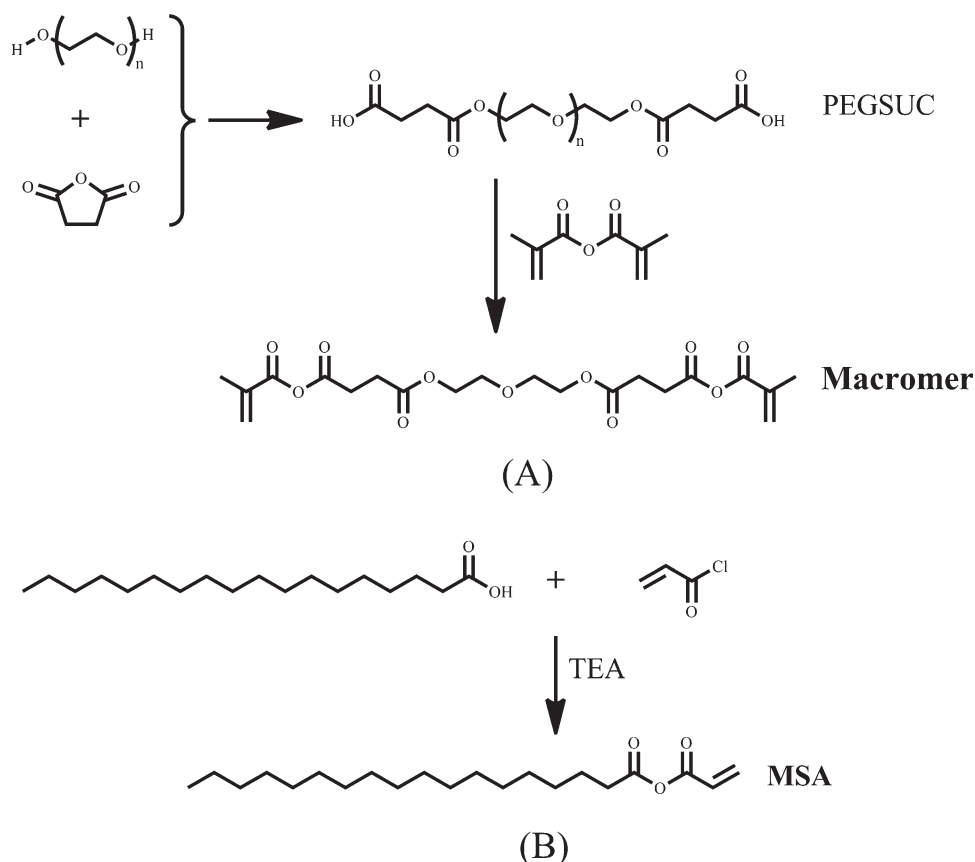
Scheme 1. Synthetic route for poly(ether-anhydride) macromer (A) and monoacrylated stearic acid (MSA) (B).

anhydride) nanocarriers that exhibit a hydrophobic core and a hydrophilic polyethylene glycol (PEG) shell with improved stability.[13] The stability and enhanced drug delivery of PEGylated poly(ether-anhydride) carriers have also been demonstrated in other previous studies.[14,15] When conjugating folate to the surface of polymeric nanocarriers, they would show not only serum stability and biodegradability but also tumor targeting ability.[16] On parenteral administration, the nanocarriers can degrade into biocompatible PEG and nontoxic acid counterpart in vivo that can be eliminated from the body as metabolites.

The degradation behavior of polymer is another parameter that influences the fate of polymeric nanocarriers in vivo and the drug delivery efficiency. For poly(ether-anhydride) nanocarriers, their degradation has been reported mainly through a surface erosion mechanism ranging from days to years.[17,18] Nevertheless, as a result of the complexity of photopolymerized poly-(ether-anhydride) network, the polymer composition, particle size, crosslinking density, and the extent of surface engineering by PEG and folate all have an effect on the degradation behavior of folate-decorated poly(ether-anhydride) nanocarriers. The aims of this study were to design novel folate-conjugated poly-(ether-anhydride) nanocarriers for delivery of a model anticancer agent, paclitaxel (PTX) and to preliminarily investigate the polymer erosion kinetics on the drug release profiles in vitro in a nonbiological medium.

MATERIALS AND METHODS

Materials

PEG (M_w = 400 Da), folate, dicyclohexylcarbodimide (DCC), tosylchloride (TsCl), N-hydroxy-succinimide (NHS), triethylamine (TEA), and hydrazine hydrate were purchased from Tianjin Guangfu Fine Chemical Research Institute (Tianjin, China). 2, 2-dimethoxy-2-phenylacetophenone (DMPA) was sourced from Sigma-Aldrich (Shanghai, China). Methacrylic anhydride (MA), acryloyl chloride, and potassium phthalimide were purchased from Aladdin (Shanghai, China). Poly(vinyl alcohol) (PVA, M_w = 6000 Da, 80% hydrolyzed) was kindly supplied by Shanxi Sanwei Group (Shanxi, China). The model drug PTX was provided by Aladdin (Shanghai, China) and coumarine-6 was purchased from Acros (Beijing, China). Dichloromethane (DCM), dimethylformamide (DMF), dimethyl sulfoxide (DMSO), 1, 2-dichloroethane, methanol, acetonitrile, diethyl ether, and toluene were purchased from Tianjin Jiangtian Fine Chemical Research Institute (Tianjin, China). They were all of analytical grade and redistilled before use.

Methods

Synthesis of Macromer and Monoacrylated Stearic Acid. Macromer (PEG-MA) was synthesized by melt-condensation of PEG disuccinate (PEGSUC) with MA as reported previously (Scheme 1).[13,17] Briefly, 10 g of PEG was dissolved in 150 mL toluene followed by azeotropic distillation at 110°C. Then 7.5 g succinic anhydride was added into the above solution and the

mixture was refluxed at 150°C for 5 h. The crude product was washed with saturated sodium bicarbonate and acidified to pH 3–4 using 5% hydrochloric acid. The product was further purified by precipitation with DCM to generate PEGSUC. PEG-MA macromers were synthesized by the reaction between PEGSUC and excess MA using the previously reported method with slight modification.[19] The reaction was performed at 90°C for 8 h under nitrogen atmosphere; the crude product was extracted twice with hexane and the solvent was removed by rotary evaporation. The obtained macromers were vacuum-dried ready for use.

Dried stearic acid (5 g) and 7.6 mL TEA were dissolved in 50 mL DCM and the mixture was maintained at 0°C for 1 h under nitrogen atmosphere. Acryloyl chloride (4.3 mL) was added dropwise to the solution and the reaction was continued for 4 h followed by filtration to remove the precipitates. The filtrate was washed with saturated sodium bicarbonate (150 mL × 2) and distilled water (150 mL × 2). The dried organic phase was evaporated under vacuum producing a viscous liquid. The final product (MSA) was precipitated twice in an ethanol/diethyl ether (3:2, v/v) solution and vacuum-dried.

Synthesis of Folate-Modified Macromer. Folate-modified macromer was synthesized via the reaction between folate-conjugated PEG (FA-PEG-OH) and MA; Folate was activated into the ester (NHS-FA) and conjugated to HO-PEG-NH$_2$ generating FA-PEG-OH and then FA-PEG-MA (Scheme 2). The conjugation began with the preparation of amino PEG (HO-PEG-NH$_2$) by Gabriel reaction based on previously published method.[20,21] Phthalimide (20 g) was dissolved in 160 mL ethanol followed by adding ca. 7.68 g KOH in methanol; the reaction was maintained at ambient temperature for 3 h and the crude product was washed with ethanol and vacuum-dried to generate potassium phthalimide (1). PEG (10 g) was dissolved in 150 mL DCM with subsequent adding 5.4 g TsCl in 20 mL TEA and the reaction was kept at ambient temperature for 18 h. The solution was extracted using 1 M HCl in triplicate followed by treating the organic phase with anhydrous sodium sulfate; the residue was dissolved in 10 mL DCM, precipitated in diethyl ether, filtered, and dried under vacuum to get tosylated PEG (2). Potassium phthalimide (9.2 g) and tosylated PEG (9.4 g) were dissolved in 150 mL DMF and the reactants were maintained at 120°C for 72 h under nitrogen (3); the crude product was dissolved in a mixture of ethanol (120 mL) and hydrazine hydrate (5 mL), refluxed at 70°C for 72 h and purified by precipitation to get a mixture of PEG derivatives. The derivatives were separated by silica gel column chromatography by using 1% TEA solution in DCM/methanol (8:1, v/v) as the eluent. As a result, HO-PEG-OH, HO-PEG-NH$_2$ could be identified by thin-layer chromatography. The product of HO-PEG-NH$_2$ was redissolved in DCM, dried under anhydrous sodium sulfate, precipitated in diethyl ether, filtered, and vacuum-dried ready for use (4). The activated ester of folate, that is, NHS-FA was synthesized according to the procedure described before.[22,23] Folate (1.0 g) was added to 40 mL DMSO containing 0.5 mL TEA and the reaction was protected against light; after 12 h the solution was mixed with 0.5 g DCC plus 0.28 g NHS; after 18 h the side-products were removed by filtration and NHS-FA was purified by precipitation in diethyl ether (5). The generation of FA-PEG-OH can be achieved by the reaction between NHS-FA (0.21 g) and equimolar NH$_2$-PEG-OH (1.0 g) in DMSO in the presence of TEA (80 μL); the mixture was stirred for 36 h under nitrogen at ambient temperature followed by precipitation with diethyl ether; the crude product was further purified by the distillation in toluene to get FA-PEG-OH (6). At last, 0.5 g FA-PEG-OH was mixed with 5 mL MA under nitrogen at 60°C; after 24 h, 40 mL diethyl ether was added to the cooled mixture to precipitate FA-PEG-MA that was vacuum-dried ready for use (7).

FTIR and ^{1}H NMR. The structures of PEGSUC, MSA, PEG-MA, FA-PEG-MA, and other intermediate products were characterized by nuclear magnetic resonance (^{1}H NMR) and Fourier transform infrared spectroscopy (FTIR). ^{1}H NMR spectra were recorded on a Bruker AVANCE series instrument (400 MHz) using TMS as internal standard. FTIR spectra were recorded on a Tensor[TM] 27 spectrometer (Bruker Optik GmbH, Ettlingen, Germany) in the 4000–400 cm^{-1} region using KBr pellets.

Drug Assay. Quantitative analysis of PTX was achieved using an Agilent 1100 high-performance liquid chromatography (HPLC) system with a UV detector. Separation was achieved at 25°C using a Kromasil C18 column (5 μm, 250 × 4.6 mm^2) (Phenomenex, Beijing, China). The mobile phase was a mixture of methanol, acetonitrile, and water (35:40:25, v/v/v) and the flow rate was 1.0 mL/min. The injection volume was 10 μL and the detection wavelength was 229 nm.

Nanocarrier Preparation. Nanocarriers were prepared by mixing the macromers and initiator in the organic phase with an external aqueous phase to form an oil-in-water (O/W) type emulsion followed by a subsequent photo-crosslinking of the macromers.[13] In brief, 0.5 g macromer and initiator DMPA (1%, w/w) were dissolved in 10 mL DCM forming the organic phase that was dispersed in 40 mL PVA aqueous solution (2.5%, w/v). The emulsion was treated by sonication for 5 min using a probe sonicator (JY88 Crusher, Ningbo Scientz Bio-tech, China) with the power output of 250 W in an ice bath. Then the O/W emulsion was exposed to a UV lamp (365 nm, 3.5 mw/cm^2) for 30 min with continuous stirring; the distance between the solution and the lamp was set at 15 cm. After removing the solvent by evaporation, nanoparticles were collected by centrifugation at 22,000 rpm for 30 min at 4°C using an Avanti J-26 XP Series High-Performance Centrifuge (Beckman Coulter, Beijing, China) and then lyophilized ready for use. Nanocarriers crosslinked by MSA were produced by adding MSA (5%, w/w) in the organic phase of the emulsion. The folate-modified nanocarriers were prepared by replacing the macromers in the organic phase with folate-modified macromers and MSA (5%, w/w). The three types of nanocarriers were abbreviated as NC, NC-MSA, NC-MSA-FA, respectively. Paclitaxel-loaded nanocarriers were generated using the same method in the presence of appropriate amount of drug in the organic phase. The drug loading was determined by HPLC.

Nanocarrier Characterization. The morphology and size of the nanoparticles were investigated by transmission electron microscopy (TEM) (JEM-100CX II, JEOL, Tokyo, Japan) at an accelerating voltage of 100 kV. The sample was prepared by wetting a carbon-coated grid with a drop of nanocarrier aqueous suspension and dried at room temperature before observation. The hydrodynamic diameter of the nanocarriers was determined by dynamic light scattering (DLS) (Mastersizer 2000, Malvern, Beijing, China) using a He-Ne laser wavelength of 633 nm and a scattering angle of 90° at 25°C.
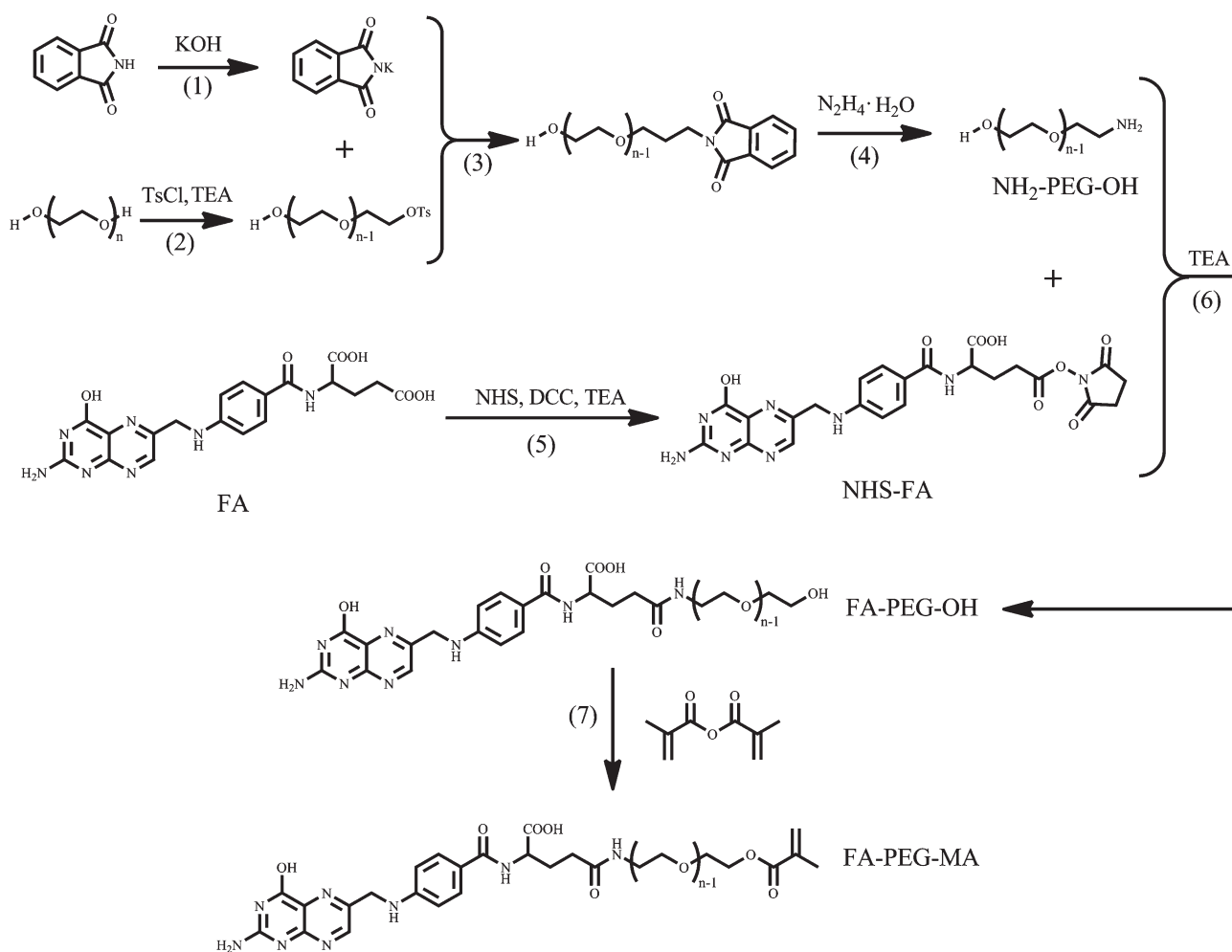
Scheme 2. Synthetic route for folate-modified poly(ether-anhydride) macromer (FA-PEG-MA).

Nanocarrier Erosion. The profile of polymer erosion was examined using our previously published method.[16] In detail, the *in vitro* erosion behavior of nanocarriers was carried out in phosphate-buffered saline (PBS, 0.1 M, pH 7.4) at 37°C. A certain weight of lyophilized nanocarriers suspended in 5 mL PBS was sealed in a dialysis bag with a molecular weight cutoff of 12,000 Da (Green Bird Co., Shanghai, China). The bag was dialyzed against 200 mL PBS medium at 37°C in a shaking water bath with a speed of 100 rpm. At predetermined intervals, samples were collected and lyophilized for measurement of weight loss.

Drug Release. The *in vitro* release profiles of PTX from nanocarriers were performed in PBS (0.1 M, pH 7.4) at 37°C. A defined amount of drug-loaded nanocarriers were suspended in 5 mL PBS and dialyzed against 200 mL of PBS (molecular weight cutoff 12,000 Da) in a shaking water bath maintained at 37°C. At predetermined intervals, 1 mL aliquot was taken out and replenished by equal volume of fresh medium. The concentration of released drug was determined by HPLC and the cumulative amount of released drug was plotted against time. PTX powder without any modification was used as the control.

Cellular Internalization. The human cervical cancer (HeLa) cells were used to study the cellular internalization of nanocarriers. HeLa cells were cultured in Dulbecco's modified eagle medium

(DMEM) supplemented with 10% fetal bovine serum under an atmosphere of 5% CO_2 at 37°C before use. The cells were seeded in 24-well plates at a density of 3×10^4 per well and allowed to attach for 24 h. Then the medium was replaced by fresh DMEM containing coumarin-6-loaded NP-MSA or NP-MSA-FA (1 mg/ mL). After 30 min of incubation, the cells were rinsed three times with PBS to clean excess nanocarriers that were not internalized. The cellular uptake of nanocarriers was analyzed and recorded using an inverted fluorescence microscope.

Statistical Analysis. Statistical analysis of data was carried out using SPSS and a statistically significant difference was determined at a minimal level of significance of 0.05. Polymer degradation and drug release data were analyzed using *t*-test or one-way ANOVA with Turkey's post hoc test.

RESULTS AND DISCUSSION

Preparation and Characterization of Nanocarriers

The generation of MSA, PEGSUC, and corresponding macromers was verified by FTIR and ^{1}H NMR analysis in our previous work.[13] Folate-modified macromer, that is, FA-PEG-MA was successfully synthesized by the reaction between FA-PEG-OH and MA, which was evidenced by the ^{1}H NMR spectrum (Figure 1). The peaks at 5.32 ppm (peak 1) and 5.73 ppm (peak
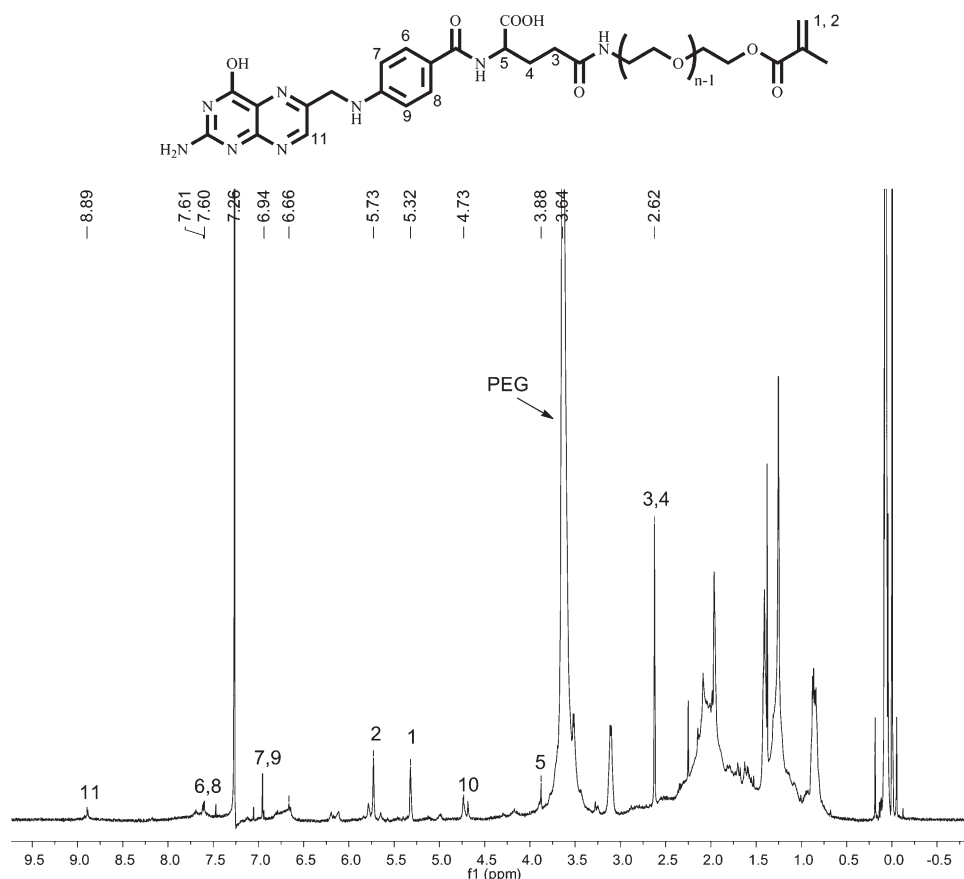
Figure 1. The ^{1}H NMR spectrum folate-modified poly(ether-anhydride) macromer (FA-PEG-MA).

2) were assigned to the vinyl group protons at the terminal of macromer, which demonstrated the conjugation of MA to FA-PEG-OH. The strong peak at 3.64 ppm was attributed to methylene protons of PEG, while the signals at 6.66–7.61 ppm corresponded to the aromatic protons of folate molecule, which proved the existence of the folate moiety in the macromer. FTIR was also used to characterize FA-PEG-MA (Figure 2). The peaks of 1100 cm^{-1} represent the vibrations of ether linkage in PEG. However, as a consequence of poor signal from C=C bond in MA (1637 cm^{-1}), such signal was not evident in the spectrum of FA-PEG-MA.

The generation of poly(ether-anhydride) nanocarriers was achieved by treating the macromers with UV irradiation followed by the evaporation of organic solvent, which was similar to the typical emulsification-solvent evaporation method technique.[24] The photopolymerization of macromers in the organic phase of the O/W emulsion was initiated by the DMPA initiator to create the poly(ether-anhydride) network that constitutes the framework of the nanocarrier. The formulation parameters including the ratio between organic and aqueous phases and the concentration of PVA stabilizer have been optimized in our previous study.[13] These factors are crucial to the physical stability of the O/W emulsion, which determines the size and size distribution of nanocarriers.

Depending on the type of macromers dissolved in the dispersed phase of the emulsion, three categories of nanocarriers were produced: NC, NC-MSA, and NC-MSA-FA; the corresponding macromers were PEG-MA, PEG-MA with MSA, FA-PEG-MA plus MSA, respectively. The hydrodynamic size (polydispersity index, PI) of placebo NC, NC-MSA, and NC-MSA-FA were 266.7 nm (0.261), 291.2 nm (0.238), and 341.8 nm (0.296), respectively. The TEM analysis concurs with the DLS results (Figure 3); the incorporation of hydrophobic MSA increased the viscosity of the organic phase leading to relatively larger O/W droplet and thus increased particle size.[13] Modifying the macromers with folate also resulted in an increase of nanocarrier diameter. This was because the presence of folate moiety extended the length of PEG spacer resulting in a bigger particle, and such phenomenon was reported in previous independent studies.[25] As expected, loading the active agent in the poly(ether-anhydride) nanocarriers increased the particle size that was determined by DLS. The diameters (PI) of drug-loaded NC, NC-MSA, and NC-MSA-FA were 315.8 nm (0.162), 362.4 nm (0.265), and 378.8 nm (0.342), respectively. To enhance drug delivery to the solid tumors via the enhanced permeability and retention effect, future work will optimize the synthesis conditions to limit the nanocarriers within 200 nm. Irrespective of the nanocarrier type, both placebo and drug-loaded nanocarriers exhibited a polydispersed size distribution. This can be explained by the nanocarrier manufacture method and the size distribution of nanocarriers was affected dramatically by the size distribution of emulsion droplet. The emulsion droplet is
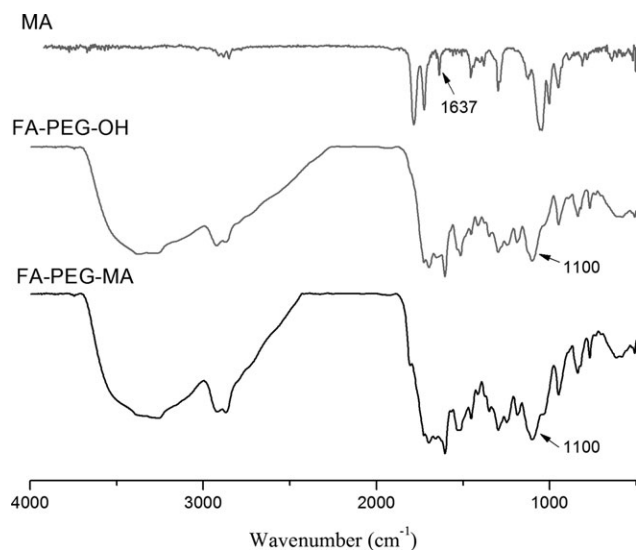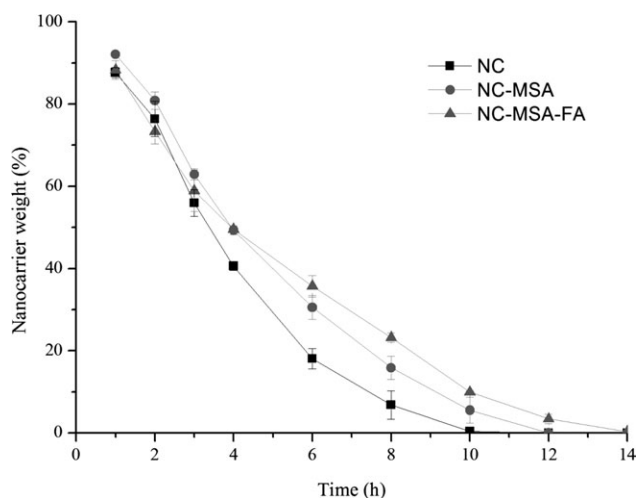
Figure 2. The FTIR spectra of MA, folate (FA)-conjugated PEG (FA-PEG-OH), and folate-modified poly(ether-anhydride) macromer (FA-PEG-MA).

Figure 4. The erosion kinetics of three types of nanocarriers: NC, NC-MSA, and NC-MSA-FA in PBS medium at 37°C.

not uniform even in the presence of PVA stabilizer because emulsion is a thermodynamically unstable system that tends to revert back to the individual phases. The mean drug loading was 17% (w/w, NC), 12% (w/w, NC-MSA), and 9% (NC-MSA-FA), respectively, with a corresponding encapsulation efficiency of 42% (NC), 67% (NC-MSA), and 43% (NC-MSA-FA).
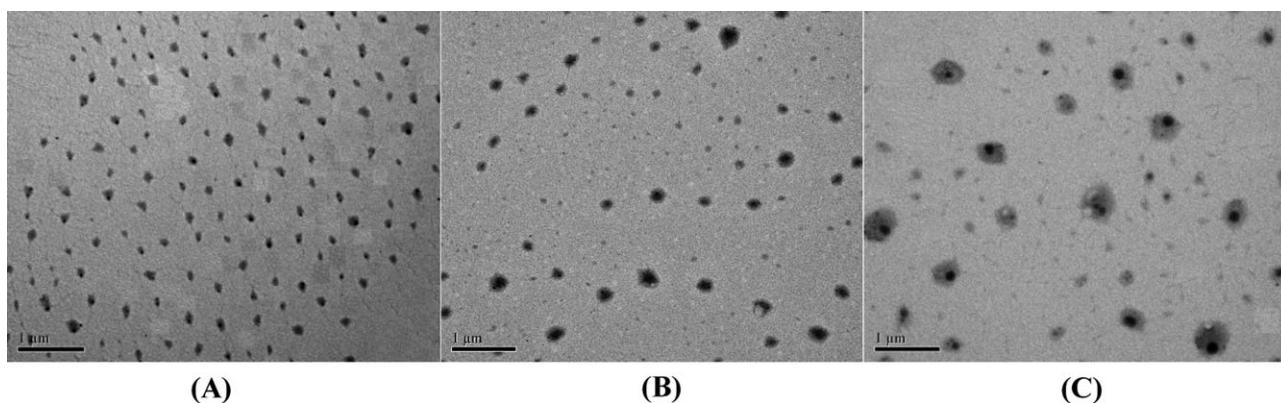
Polymer Erosion and Drug Release

The erosion profiles of the crosslinked poly(ether-anhydride) nanocarriers were investigated in PBS (0.1 M, pH 7.4) at 37°C (Figure 4). The nanocarriers obtained in this study were biodegradable and the degradation products include PEG, poly(methacrylic acid), and succinate, which were nontoxic and biocompatible. All of them could be excreted directly from various metabolic pathways. All three types of nanocarriers (NC, NC-MSA, and NC-MSA-FA) were eroded thoroughly within ca. 12 h and the rate of erosion for NC-MSA and NC-MSA-FA was relatively lower compared to that of NC. For example, after 6 h, the percentage of nanocarrier residue weight was $18.0 \pm 2.5\%$, $30.5 \pm 2.9\%$, and $35.7 \pm 2.6\%$, for NC, NC-MSA, and NC-

MSA-FA, respectively ($P < 0.05$). The mean steady rate of polymer erosion was 43.6 $h^{-1/2}$ (NC), 42.0 $h^{-1/2}$ (NC-MSA), and 35.7 $h^{-1/2}$ (NC-MSA-FA). Although the photo-crosslinked poly(ether-anhydride) network is a complex system, the erosion of photopolymerized particles is primarily controlled by two factors based on previous investigation[17]; one is the crosslinking density and the other is the hydrolytic susceptibility (i.e., wettability). The polymer erosion is speeded under the circumstance of low crosslinking density and high hydrolytic susceptibility. Therefore, the relative slow degradation of NC-MSA and NC-MSA-FA was a result of the condensed core that consisted of the homopolymers of macromer, MSA, and the copolymer of macromer and MSA. The presence of folate in the nanocarrier surface (i.e.,NC-MSA-FA) partly shields the interaction between hydrophilic PEG and water creating a less hydrophilic surface compared to that of NC-MSA. The diminished surface wettability for NC-MSA-FA could retard the entry of water into the nanocarrier interior and thus delay the hydrolysis of anhydride resulting in comparatively slower polymer erosion. Consecutive analysis of the dialyzed sample via gel permeation chromatography and DLS would further get the degradation profile of the polymers.
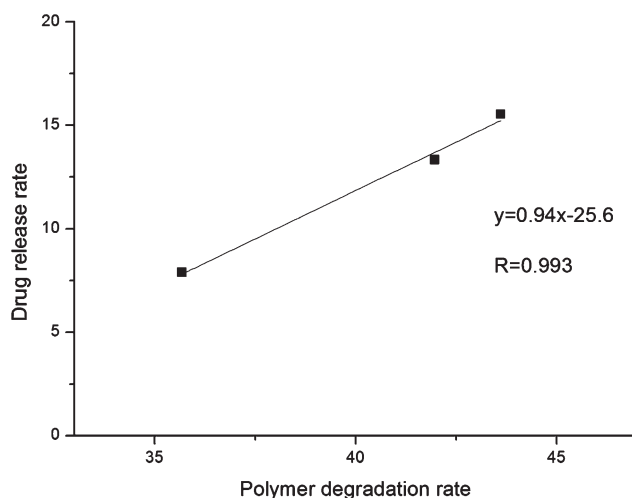

Figure 3. The TEM image of three types of photo-crosslinked poly(ether-anhydride) nanocarriers: NC (A), NC-MSA (B), and NC-MSA-FA (C).
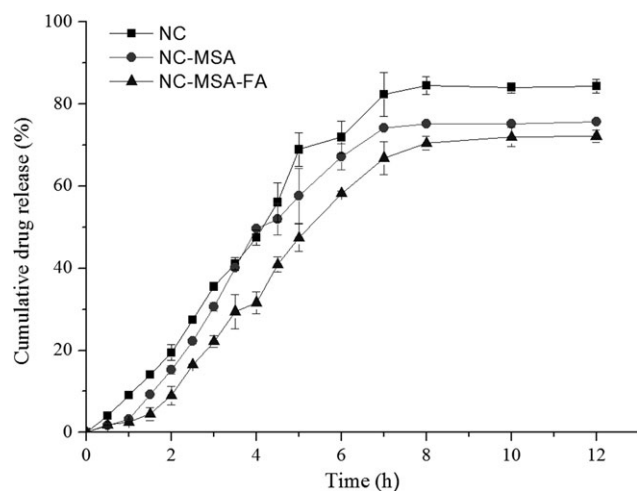
Figure 5. The *in vitro* release profiles of PTX from three types of nanocarriers: NC, NC-MSA, and NC-MSA-FA.

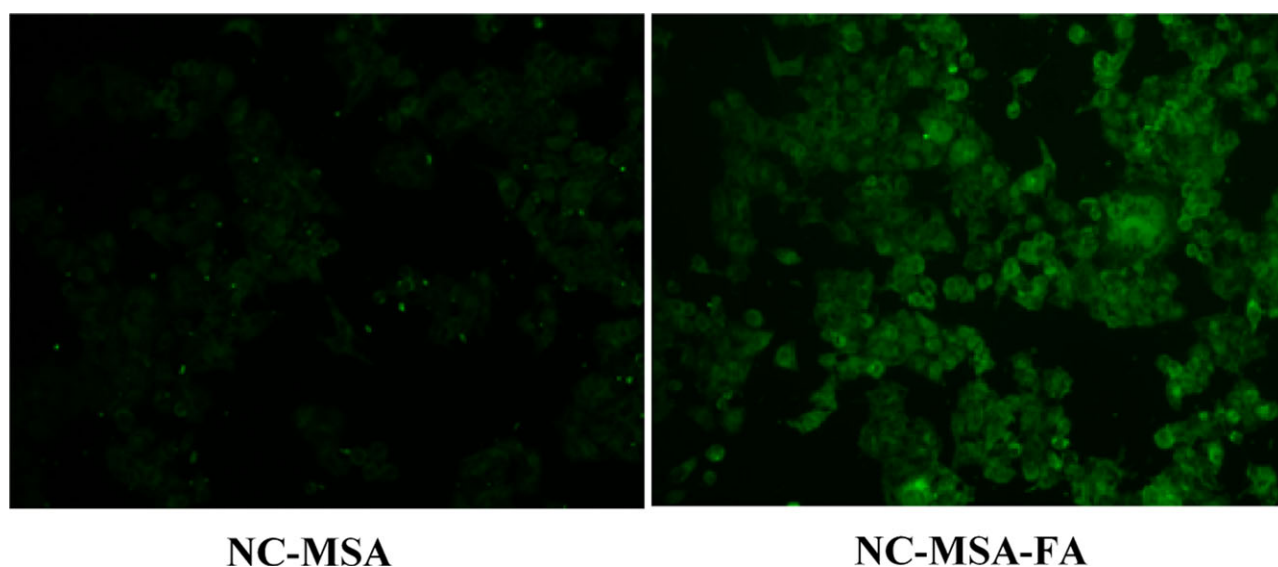**Figure 6.** The correlation between polymer erosion rate and drug release rate.

The *in vitro* drug release profiles of three types of nanocarriers were investigated in PBS (0.1 M, pH 7.4) at 37°C (Figure 5). The drug was released rapidly from all samples within 6 h, after which the release profile got plateaued. At 8 h, 84.4 $\pm$ 2.1%, 75.1 $\pm$ 0.5%, and 70.5 $\pm$ 1.7% of drug was released into the release medium from NC, NC-MSA, and NC-MSA-FA, respectively ($P < 0.05$). The steady rate of drug release was 15.5 h^{-1} (NC), 13.2 h^{-1} (NC-MSA), and 7.9 h^{-1} (NC-MSA-FA) based on the Higuchi model. The presence of MSA slowed down PTX release from NC-MSA and NC-MSA-FA compared to that from NC because of the interaction between hydrophobic MSA and drug.[13] However, in contrast to NC-MSA, the wettability of NC-MSA-FA was weakened due to the presence of hydrophobic FA at nanocarrier surface. This would delay the entry of water into the nanocarrier interior and thus hinder the drug dissolution and release. The size of nanocarrier also played a role in

determining the drug release profile as the high surface area of smaller nanocarriers would offer shorter drug diffusion distance thus leading to more rapid drug release. This agreed well with the drug release data and the drug release rate from three types of nanocarriers was consistent with the size of nanocarriers; the release rate from smallest NC ranked the highest, whereas the release rate from the largest NC-MSA-FA is the lowest. Further work on the drug release in a biologically relevant medium, for example, plasma would add value to the *in vivo* application of such nanocarriers.

It is true that both nanocarrier size and polymer erosion can influence the drug release. Nevertheless, in current study the erosion of polymer network is dominant in determining the drug release profile. This can be supported by the surprising matching of time scales of polymer erosion and drug release. At 6 h, more than 50% of polymer was hydrolyzed and meanwhile

Figure 7. Cellular internalization of poly(ether-anhydride) nanocarrier without (NC-MSA) and with (NC-MSA-FA) folate modification. [Color figure can be viewed in the online issue, which is available at wileyonlinelibrary.com.]

the drug release profile began to get plateaued. The correlation between polymer erosion and drug release was further demonstrated by the steady rate of erosion and release (Figure 6). Plotting drug release rate against polymer erosion rate generates a perfect straight line with a correlation coefficient of more than 0.99. However, only three types of nanocarriers were presented in this study, future work would expand such relationship to other similar nanocarriers.

To investigate the targeting effect of folate-modified nanocarriers, the cellular internalization of nanocarriers was examined using the fluorescence (coumarin-6) as the marker under inverted fluorescence microscope. As shown in Figure 7, coumarin-6-contained NC-MSA-FA nanocarrier showed higher fluorescence intensity compared to NC-MSA indicating a more sufficient interaction of folate-modified nanocarriers with the HeLa cell membranes. This was attributed to the conjugation of folate moiety to the carrier surface, which promoted the folate receptor-mediated endocytosis.[26] This concurs well with the overexpression of folate receptor alpha in HeLa cells based on a previous investigation.[27] In future studies, the use of confocal laser scanning microscopy with cell membrane and nucleus labeling would generate the cell update profile of these nanocarriers. The results demonstrated that the novel folate-modified poly(ether-anhydride) nanocarriers might play an active role in the targeted delivery of anticancer drugs.

CONCLUSIONS

Biodegradable folate-modified poly(ether-anhydride) nanocarriers with a hydrophobic photo-crosslinked core and a hydrophilic PEG shell were prepared. The nanocarriers with or without folate moiety could degrade rapidly in PBS within ca. 12 h at physiological temperature via a hydrolysis mechanism. The presence of MSA in the carrier increased the crosslinking density and slightly decreased the erosion rate, whereas the conjugation of folate to the carrier surface diminished the carrier wettability and thus slowed the degradation process. The PTX-loaded nanocarrier exhibited a rapid drug release profile that matched well with the time scale of nanocarrier erosion, indicating the dominant role of the degradation of poly(ether-anhydride) network in drug release. Folate-modified nanocarriers showed an enhanced targeting effect to HeLa cells compared to those without folate, suggesting that such nanocarriers might be a promising system for site-specific anticancer drug delivery and targeting.

ACKNOWLEDGMENTS

REFERENCES

1. Torchilin, V. P. *AAPS J.* **2007**, *9*, 128.

2. Pamujula, S.; Hazari. S.; Bolden, G.; Graves, R. A.; Chinta, D. D.; Dash, S.; Kishore, V.; Mandal, T. K. *J. Pharm. Pharmacol.* **2012**, *64*, 61.

3. Reddy, R. H. *J. Pharm. Pharmacol.* **2005**, *57*, 1231.

4. Greish, K. *J. Drug Target.* **2007**, *15*, 457.

5. Byrne, J. D.; Betancourt, T.; Brannon-Peppas, L. *Adv. Drug Delivery Rev.* **2008**, *60*, 1615.

6. Ling, S. S.; Yuen, K. H.; Magosso, E.; Barker, S. A. *J. Pharm. Pharmacol.* **2009**, *61*, 445.

7. Lu, Y. J.; Low, P. S. *Adv. Drug Delivery Rev.* **2002**, *54*, 675.

8. Peer, D.; Karp, J. M.; Hong, S.; Farokhzad, O. C.; Margalit, R.; Langer, R. *Nat. Nanotechnol.* **2007**, *2*, 751.

9. Torchilin, V. *Eur. J. Pharm. Biopharm.* **2009**, *71*, 431.

10. Yoo, J. W.; Chambers, E.; Mitragotri, S. *Curr. Pharm. Des.* **2010**, *16*, 2298.

11. Gaucher, G.; Dufresne, M. H.; Sant, V. P.; Kang, N.; Maysinger, D.; Leroux, J. C. *J. Controlled Release* **2005**, *109*, 169.

12. Drummond, D. C.; Meyer, O.; Hong, K.; Kirpotin, D. B.; Papahadjopoulos, D. *Pharmacol. Rev.* **1999**, *51*, 691.

13. Wang, Z.; Cai, Z.; Guo, Q. *Macromol. Symp.* **2010**, *297*, 167.

14. Fiegel, J.; Fu, J.; Hanes, J. *J. Controlled Release* **2004**, *96*, 411.

15. Tang, B. C.; Fu, J.; Watkins, D. N.; Hanes, J. *Biomaterials* **2010**, *31*, 339.

16. Zhu, J.; Zhou, Z.; Yang, C.; Kong, D.; Wan, Y.; Wang, Z. *J. Biomed. Mater. Res. A* **2011**, *97*, 498.

17. Kim, B. S.; Hrkach, J. S.; Langer, R. *J. Polym. Sci.* **2000**, *38*, 1277.

18. Burkoth, A. K.; Anseth, K. S. *Biomaterials* **2000**, *21*, 2395.

19. Tarcha, P. J.; Su, L.; Baker, T.; Langridge, D.; Shastri, V.; Langer, R. *J. Polym. Sci.* **2001**, *39*, 4189.

20. Furukawa, S.; Katayama, N.; Izuka, T.; Urabe, I.; Okada, H. *FEBS Lett.* **1980**, *121*, 239.

21. Yokoyama, M.; Okano, T.; Sakurai, Y.; Kikuchi, A.; Ohsako, N.; Nagasaki, Y.; Kataoka, K. *Bioconjugate Chem.* **1992**, *3*, 275.

22. Patil, Y. B.; Toti, U. S.; Khdair, A.; Ma, L.; Panyam, J. *Biomaterials* **2009**, *30*, 859.

23. Singh, P.; Gupta, U.; Asthana, A.; Jain, N. K. *Bioconjugate Chem.* **2008**, *19*, 2239.

24. Watts, P. J.; Davies, M. C.; Melia, C. D. *Crit. Rev. Ther. Drug Carrier Syst.* **1990**, *7*, 235.

25. Esmaeili, F.; Ghahremani, M. H.; Ostad, S. N.; Atyabi, F.; Seyedabadi, M.; Malekshahi, M. R.; Amini, M.; Dinarvand, R. *J. Drug Target.* **2008**, *16*, 415.

26. Yoo, H. S.; Park, T. G. *J. Controlled Release* **2004**, *100*, 247.

27. Chan, S. Y.; Empig, C. J.; Welte, F. J.; Speck, R. F.; Schmaljohn, A.; Kreisberg, J. F.; Goldsmith, M. A. *Cell* **2001**, *106*, 117.